Water on the outside of carbon nanotube bundles

M. C. Gordillo*

Departamento de Ciencias Ambientales, Facultad de Ciencias Experimentales, Universidad Pablo de Olavide, Carretera de Utrera km 1, 41013 Sevilla, Spain

J. Martí[†]

Departament de Física i Enginyeria Nuclear, Universitat Politècnica de Catalunya, B5-206 Campus Nord UPC, 08034 Barcelona, Catalonia, Spain

Molecular-dynamics simulations of water on the outer surface of a bundle of carbon nanotubes are reported. We observed a first-order phase transition from a low-density regime in which the water molecules are confined in the grooves between tubes and a high-density one, characterized by adsorption of water on all the surface exposed. Both phases could be experimentally detected by the differences in the locations of the main peaks of their infrared spectra.

I. INTRODUCTION

Much work has been recently devoted to the study of carbon nanotubes (CN's) which are long and extremely narrow cylinders whose walls are made of graphite sheets rolled up over themselves.[1] Nanotubes are interesting in their own way, for instance, because of their electronic properties and also because they allow the realization of a quasi-one-dimensional environment for the materials absorbed inside. In particular, the case of water inside such narrow cylinders has recently received some consideration, with several simulation studies of classical water confined in CN's,[2–4] or in more idealized environments.[5] However, to let any substance enter a CN, it has to be opened by chemical or other means, since in their naturally occurring form both ends are closed by caps. It is also known that CN's usually associate together to form bundles, which means that water or other substances have to stay on the outer surface of the bundle, or if they are small enough, in the internal channels between nanotubes. Since the maximum radius of such interchannels from the center of the channel to the center of the carbon site is 3.5 Å,[6] and that radius is slightly larger than the oxygen-carbon minimum distance, water molecules are too large for this last possibility. For this reason, it could be interesting to know how water behaves when absorbed in the outer part of the bundle, the only surface exposed. This is an interesting substrate, that should partake of the characteristics of graphite, but presents some interesting effects due to its curvature, as has already been reported in the case of some gases.[7]

II. COMPUTATIONAL DETAILS

In this work we report molecular-dynamics simulations of water in the outer surface of a bundle of CN's at different temperatures ranging from 250 to 325 K and at several densities. The water molecules were described by a flexible SPC model[8] including intramolecular interactions modeled by harmonic and Morse-type terms. Such potential is able to reproduce the basic features of the experimental bands in the infrared spectrum of bulk water. The interaction between a water molecule and the CN is the averaged one given by Cole and co-workers,[9] with force parameters obtained from Lorentz-Berthelot rules: $\sigma_{OC} = 3.28$ Å, $\sigma_{HC} = 2.81$ Å, $\epsilon_{OC} = 0.3890$ kJ/mol, $\epsilon_{HC} = 0.129$ kJ/mol (see Ref. 2 for more details). Very recently,[10] an extensive comparison among different water-graphite potentials has been carried out. Since a CN is basically a cylindrical graphite sheet, those comparisons should be relevant to our problem. Our model is in the middle part of the tables for the two properties checked out, the graphite-water interaction, and the wetting angle of water drops on top of a sheet of graphite. The single water molecule-carbon interaction energy obtained with our parameters is -9.70 kJ/mol, versus energies ranging from -5.07 to -16.54 kJ/mol for other potential models. In Ref. 10 is also computed the water-graphite contact angle, which determines the wetting phenomena. In our case, that angle is $\sim 60°$, indicating that the wetting takes place. The other potentials render values between $0°$ and $\sim 140°$. The experimental angles (Ref. 10 and references therein) are between $\sim 90°$ and $\sim 40°$. In both cases, our potential is just in the middle of the possible values. According to all that water should wet graphite and also the surface of a carbon nanotube. Moreover, it has been experimentally found that water can be adsorbed inside chemically treated CN's.[11] However, this does not mean that carbon nanotubes are soluble in water. The CN-CN interactions are strong enough to prevent the breakup of the bundle when surrounded by water. On the other hand, when exposed to moderate quantities of fluid, one would expect water to adsorb on the outer surfaces of the tubes.

Our simulation cell was a cube of 34 Å of side, wide enough to have two parallel (10,10) tubes (those with a radius of 6.8 Å) with longitudinal axes along the z axis. This arrangement implies the existence of two parallel depressions, separated by 17 Å, in between the tubes, that we termed grooves. The tubes are taken to be rigid in the simulations, since the consideration of carbon mobility has little effect on the computed properties.[10] At the beginning of every simulation, all the water molecules are located forming a homogeneous flat layer at 9 Å from the center of the CN.
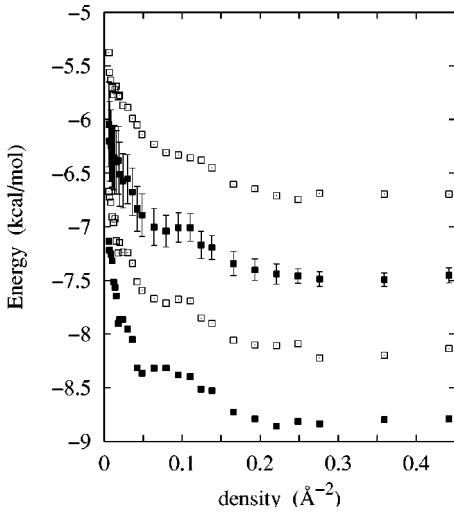
FIG. 1. Total energy per water molecule as a function of density. Top to bottom: 325 K (upper open squares), 298 K (upper full squares), 273 K (lower open squares), and 250 K (lower full squares).

After an equilibration period of about 50 ps, none of the water molecules remained in a hypothetical gas phase above the tubes, all of them being adsorbed in the outer surface of the bundle. The thermodynamical and dynamical properties presented here were collected from runs of 0.1 ns each. Periodic boundary conditions were considered. More details about how the calculations are made can be found elsewhere.[2]

III. DISCUSSION

One of the primary outputs of any molecular-dynamics simulation is the energy. In Fig. 1 we represent that magnitude as a function of the surface density. To calculate that density, we divided the number of molecules in the simulation cell by the square of its side, i.e., we did not take into account the total exposed surface of the cylinders. To go from a number to the other, we have only to multiply for the appropriate constant factor. The curves correspond, from top to bottom, to 325, 298, 273, and 250 K. The error bars were displayed only for the case of room temperature, being similar in the other cases and omitted for simplicity. We also observe that there is always a kind of a plateau for energies in between the densities of ~ 0.03 and ~ 0.11 Å^{-2} (in the above-mentioned units). There is no doubt that, at least, there is a change in the slope of the energy around those densities for all temperatures, which could indicate a transition between a low-density phase and a high-density one. It has to be pointed out that at least one liquid-solid phase transition at 235 K has recently been found for water adsorbed inside single-walled carbon nanotubes.[11]

Nevertheless, to check the possibility of a phase transition what we need is not the energy but the free energy. This magnitude cannot be directly obtained from a molecular-dynamics simulation, but since we have results for several temperatures, we can estimate it by means of the thermodynamic relationship between the energy and the free energy.

The strategy will be to propose a reasonable form for the free energy as a function of temperature and density (its natural variables) and to deduce the corresponding expression for the energy by means of[12]

$$E = -T^2 \frac{\partial (F/T)}{\partial T}.$$

(1)

The chosen form for the free energy was

$$F = -\frac{3}{2} NkT \ln \frac{2\pi MkT}{h^2} - NkT \ln \frac{Ve}{N} - NkT \ln \frac{\pi^{1/2}}{\sigma}$$

$$- \frac{1}{2} NkT \ln \frac{T^3}{\Theta_A \Theta_B \Theta_C}$$

$$+ Nk \sum_{j=1}^{3n-6} \left(\frac{\Theta_{vj}}{2} + T \ln[1 - \exp(-\Theta_{vj}/T)] \right)$$

$$+ \sum_{i=0}^{3} \sum_{j=1}^{3} b_{ij} \rho^i T^{1-j}.$$

(2)

The first five terms are those corresponding to an ideal polyatomic gas, being the last sum of the correction added. It has been chosen in such a way that in the limit of infinite dilution and infinite temperature ($\rho \to 0$ and $T \to \infty$), we recover the expression of the ideal gas plus a term (b_{01}) that could be associated with the tube-water interaction. The symbols have the following meanings: V, volume of the simulation cell; N, number of water molecules; M, molecular mass of water; k, Boltzmann constant; h, Planck constant; $\Theta_{A,B,C}$, characteristic rotational temperatures; σ, symmetry number for water; Θ_{vj}, characteristic vibrational temperature for the jth degree of freedom; ρ, density of the water molecules in the simulation cell in Å^{-2}. Given the values of the characteristic vibrational temperatures (all above 2000 K),[13] it is very reasonable to neglect the logarithmic term inside the corresponding sum at the temperatures considered in this work. We have then a constant vibrational contribution that could be included in the b_{01} (constant) term of the last sum.

The form for the energy that results from applying the definition given in Eq. (1) to the above free energy is

$$E = 3NkT + \sum_{i=0}^{3} \sum_{j=1}^{3} j b_{ij} \rho^i T^{1-j}.$$

(3)

We made two least-squares fits to this expression, one for densities between 0.03 and 0.11 Å^{-2} and another for densities greater than 0.11 Å^{-2}. The b_{ij} coefficients are given in Table I and the results for the free energy are displayed in Fig. 2. There, full lines represent the free energy for the high-density regime and dashed lines the same for the low-density one. From top to bottom, we have the results for 250, 273, 298, and 325 K in both sets of curves. The abscissae are the inverse of the densities given in Fig. 1, which allow the drawing of the corresponding double-tangent lines in the Maxwell construction (dotted lines), and to obtain the equi-

TABLE I. Coefficients of the least-squares fit of the energy per water molecule. Phase I: 0.03 Å$^{-2}<\rho<0.11$ Å^{-2}; phase II: $\rho<0.11$ Å^{-2}.

	Phase I	Phase II
χ^2/ν	0.0405	0.1733
b_{01}	15.3463	29.4676
b_{11}	-1.1580×10^3	-3.8352×10^2
b_{21}	2.4976×10^4	1.5423×10^3
b_{31}	-1.5430×10^5	-1.8374×10^3
b_{02}	-1.2898×10^4	-1.9760×10^4
b_{12}	7.2273×10^5	2.1314×10^5
b_{22}	-1.5442×10^7	-8.6422×10^5
b_{32}	9.4551×10^7	1.0341×10^6
b_{03}	1.8301×10^6	2.5606×10^6
b_{13}	-1.1655×10^8	-3.0374×10^7
b_{23}	2.4221×10^9	1.2301×10^8
b_{33}	-1.4584×10^{10}	-1.4703×10^8

librium densities. The minima are very similar in all cases, corresponding to densities around 0.18 and 0.036 Å^{-2} for both regimes. That means that we have a high-density phase for $\rho>0.18$ Å^{-2} and a low-density one for $\rho<0.036$ Å^{-2}. Further, any system with water density in between would be unstable with respect to the formation of the two mentioned phases.

The characterization of both phases is done with the help of Fig. 3. We show here the density in g/cm^3 of water for $\rho=0.0362$ Å^{-2} (lower part of the figure) and the same magnitude for 0.193 Å^{-2} (upper part). Both densities are computed in the xy plane, perpendicular to the z axis, along which both tubes lie. The outer lines correspond in both figures to the density contour of 1 g/cm^3. Each inner line indicates then progressively greater densities from 2 to 7 g/cm^3, and the last one is the contour of 8 or more g/cm^3. The plots are drawn for $T=250$ K, but they are very similar in all the
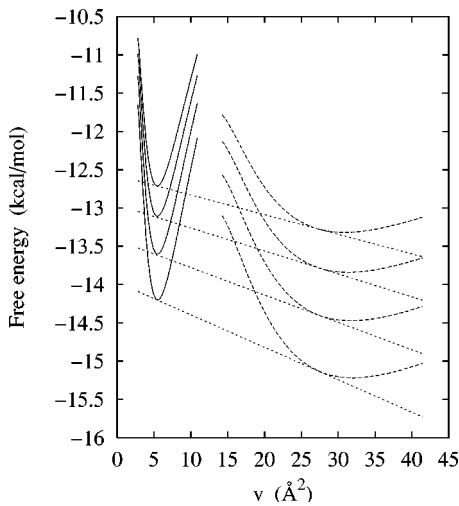

FIG. 2. Free energy per molecule as a function of inverse density. From top to bottom: 250, 273, 298, and 325 K for both sets of curves.
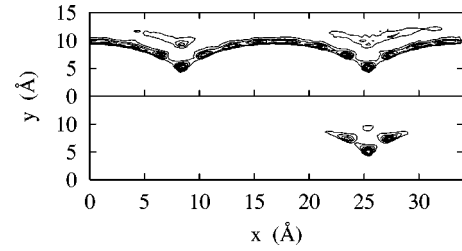

FIG. 3. Density contour plots in the XY plane for the densities of $\rho=0.0362$ Å^{-2} (phase I, bottom) and $\rho=0.193$ Å^{-2} (phase II, top).

other cases. From this figure, we can see immediately that the low-density regime (phase I) corresponds to a situation in which the molecules are confined to only one of the two grooves in a triangular pattern. On the other hand, in the high-density regime (phase II), water is adsorbed more or less homogeneously on all the surface of the tubes. We also checked the possibility of the existence of another phase for densities lower than 0.03 Å^{-2} by following the same process described above, but we got only a metastable state characterized for a single row of molecules isolated in one groove.

Given the above described phases, one could think of experimental ways to detect them. The flexible model of water employed in our simulations allows a calculation of spectral densities that can be directly related with experimental measures of infrared spectra. In particular, it has been shown that the positions of the experimental spectral bands can be calculated by Fourier transforming the molecular velocity autocorrelation functions.[3] The positions of the band maxima are directly comparable to experiments.[14] Hence we have calculated the positions of the main peaks (rotation, bending, stretching) derived from molecular-dynamics simulations in the two regimes of interest. The results are given in Table II. The temperature in all cases is 298 K. For the sake of comparison, we also included simulation results for other experimental situations. Both phases exhibit the splitting of the stretching band common to absorption inside nanotubes[3] and to a water monolayer close to a flat graphite surface.[15] However, the second peak appears at much higher wave numbers for phase I than in any other situation, even in the case in which water is allowed inside the tubes. In phase II this band is not very far from that of the monolayer case. Something

TABLE II. Positions of the main peaks in the computed spectral densities. The first two cases correspond to phase I and the third one to phase II. See text for further details. All values are given in cm^{-1}. Estimated statistical uncertainties are around 10 cm^{-1} for all values.

System class	$\omega_{\text{Rot.}}$	$\omega_{\text{Bend.}}$	$\omega_{\text{Stretch.I}}$	$\omega_{\text{Stretch.II}}$
$\rho=0.03$ Å^{-2}	405	1600	3390	3690
$\rho=0.036$ Å^{-2}	410	1605	3400	3685
$\rho=0.193$ Å^{-2}	475	1618	3405	3635
Water inside a (10,10) tube	448	1615	3412	3657
Water monolayer	470	1620	3421	3628
Bulk	491	1660	3382	

similar can be said of the bending peaks: there is a clear signature for one of the regimes (phase I; ω_b ~ 1600 cm^{-1}), but not for the other one, since a wave number of ~ 1620 cm^{-1} could correspond to phase II, to water on graphite or to water inside the tubes. However, the value in the latter case is clearly different from the bulk one. The rotational band located at around 400 cm^{-1} give similar clues: phase I and phase II are different enough, but this last one could be mistaken for water in a monolayer, although not inside the tubes or in bulk. We can say that phase I could be easily detected by means of a IR spectrum, but to do the same with phase II there should not be any graphite present.

IV. CONCLUSIONS

We performed molecular-dynamics simulations of water on the outside part of a bundle of carbon nanotubes. We found two interesting surface phases. The first of them is characterized by the presence of water in one groove of the tube bundle (phase I). For increasing density, a first-order phase transition occurs leading to a second phase of the system. This is characterized by the presence of water molecules filling the whole outer surface of the nanotube bundle (phase II). That pair of phases could be experimentally detected by means of IR spectroscopy due to the neatly distinguishable spectral signatures with the rotational-vibrational regions for each phase.

*Electronic address: cgorbar@dex.upo.es

†Electronic address: jordi.marti@upc.es

[1] R. Saito, G. Dresselhaus, and M.S. Dresselhaus, *Physical Properties of Carbon Nanotubes* (Imperial College, London, 1998).

[2] M.C. Gordillo and J. Martí, Chem. Phys. Lett. **329**, 341 (2000).

[3] J. Martí and M.C. Gordillo, Phys. Rev. B **63**, 165430 (2001).

[4] G. Hummer, J.C. Rasaiah, and J.P. Noworyta, Nature (London) **414**, 188 (2001).

[5] R. Allen, S. Melchionna, and J.P. Hansen, Phys. Rev. Lett. **89**, 175502 (2002).

[6] J. Tersoff and R.S. Ruoff, Phys. Rev. Lett. **73**, 676 (1994).

[7] M.M. Calbi, M.W. Cole, S.M. Gatica, M.J. Bojan, and G. Stan, Rev. Mod. Phys. **73**, 857 (2001).

[8] J. Martí, J.A. Padró, and E. Guàrdia, J. Mol. Liq. **62**, 17 (1994).

[9] G. Stan and M.W. Cole, Surf. Sci. **395**, 280 (1997).

[10] T. Werder, J.H. Walther, R.L. Jaffe, T. Halicioglu, and P. Koumoutsakos, J. Phys. Chem. B **107**, 1345 (2003).

[11] Y. Maniwa, H. Kataura, M. Abe, S. Suzuki, Y. Achiba, H. Kira, and K. Matsuda, J. Phys. Soc. Jpn. **71**, 2863 (2002).

[12] M.C. Gordillo and D.M. Ceperley, Phys. Rev. B **58**, 6447 (1998).

[13] D.A. McQuarrie, *Statistical Mechanics* (Harper and Row, New York, 1976).

[14] J. Martí, E. Guàrdia, and J.A. Padró, J. Chem. Phys. **101**, 10 883 (1994).

[15] M.C. Gordillo and J. Martí, J. Chem. Phys. **117**, 3425 (2002).